No. 243 (84-37)

POPULATION DYNAMICS OF "RED TIDE" ORGANISMS IN EUTROPHICATED COASTAL WATERS

by

Saburo IKEDA
and
Michio KISHI

August 1984

POPULATION DYNAMICS OF "RED TIDE" ORGANISMS IN EUTROPHICATED COASTAL WATERS-- Numerical Experiment of Phyoplankton Bloom in The East Seto Inland Sea, Japan

Saburo Ikeda* Institute of Socio-Economic Planning
University of Tsukuba

Michio Kishi** Ocean Research Institute
University of Tokyo

Abstract

A system of simulation models on the outbreak of "red tide", a large scale of phytoplankton bloom, is developed by identifying a model structure based on the marine ecological and hydrological conditions in the East Seto Inland Sea, Japan. The models consists of two parts. One is to determine hydraulic conditions of water movements in the sea. The other is to calculate biological interactions among red tide organisms and nutrients under the diffusive and advective transportation associated with the calculated water movement.

The comparison between the simulated results by our models and the observed biological or physical data on "red tide" has shown that: i) the amount of nutrients and oceanographic characteristics are basic factors for a rapid increase of phytoplankton population, iii) the alternate migration of both phyto- and zooplanktons in the vertical direction according to a light/dark cycle causes a dense phytoplankton population in the upper layer, and iii) the tidal current plus water movement induced by the wind has a great impact on phytoplankton dynamics.

*) Sakura, Ibaraki 305, Japan

**) 1-15-1 Minamidai, Nakano, Tokyo 164, Japan

1. INTRODUCTION

This paper is concerned with the identification of a model structure of phytoplankton dynamics associated with the outbreak of "red tide" in coastal water area. "Red tides" are phenomena which are often observed in summer in such an eutrophicated sea area that has excessive inflows of nutients. The sea water is reddishly colored by an unusual increase of phytoplankton population. Recent studies have shown that the oceanographic characteristics of coastal waters have also strong influences on the generation mechanism of "red tide" in such a semi-closed sea area as the Harima-Sea located at the western part of the Seto Inland Sea (Iizuka 1980, Yanagi 1982 and Okaichi 1983, 1984). This sea is shallow (the average depth is about 30 meters) and the water is not easily interchanged with that of the outer sea area. It is also surrounded by highly industrialized and urbanized regions such as Osaka, Kobe, Harima and other industrial bases. Consequently it has suffered from much inflows of nutrients and other pollutants from industrial and domestic drainages, as well as from the heavy sea traffic (See Figure 1).

A large scale of "Chattonella antiqua" red tide (a major species of phytoplankton which blooms in summer and may cause damages to fishery and recreational amenities) has appeared since the late 1960s. For example, in 1978, a number of the dense patches of the "Chattonella antiqua" blooms were observed in the most part of the northern Harima-Nada and the highest cell number of the population amounted to 5,840/ml on July 28 (Okaichi 1983). It is now a common understanding among researchers on the "red tide" problem that the mechanism of "red tide" outbreak involves a complicated interactions among biological specifics of the red tide organisms, local oceanographic characteristics, the inflows of nutrients, the climatic

factors, and so on. To identify such a complicated model structure of "red tide" in the Harima-Sea, we use the systems approach by which we elaborate a structure of marine ecological-hydrological system from a simple one to the more complex one.

This paper consists of three sections. The first one is concerned with a simple structure of phytoplankton dynamics in one-dimensional space with the consideration of phytoplankton's vertical movement. The second one deals with a simple eco-physical structure of the two-dimensional model in view of wind-induced movement of sea water in order to evaluate the effect of upwelling to the primary production. The third one is devoted to a more realistic structure of the three-dimensional model which has six ecological compartments in the tidal current plus the wind-induced water movement of two levels (layers): two kinds of "phytoplanktons", "zooplankton", "nitrogen" and "phosphorus" as nutrients for phytoplankton's growth, and "detritus" as the dissolved organic matters in the sea water. By means of numerical experiments based on our three models, we will try to find out some specific combinations of the oceanographic and ecological factors that are supposed to cause a "red tide" in the Harima-Sea.

2. ONE-DIMENSIONAL MODEL

2.1 Model Structure

This simple model is constructed to examine whether or not the up-and-down motion of both zooplankton and phytoplankton is essential to the formation of "red tide". In addition to the factors of nutrient uptaking for phtosynthesis or physical accumulation for forming a plankton patch, the prey-predator interaction between phyto- and zooplanktons plays an important role in terms of keeping a high growth rate of phytoplankton population. It seems, therefore, to be critical to see the effect of

interaction through the up-and-down movements of phyto- and zooplanktons on the prey-predator relationship.

The relationship of biological processes is illustrated in Figure 2 in which Chattonella antiqua is a primary producer, P, (this is a major species that causes "red tide" in the Harima-Nada), and Paracalanus parvus is a zooplankton, Z, as a representative species in this area, and $PO_4^{-}P$ is a nutrient, E. The photosynthetic and grazing functions are approximated by the type of Michaelis-Menten relationship as follows:

$$\frac{dP}{dt} = \frac{V_m E}{K_s + E} P \tag{2.1}$$

$$\frac{dZ}{dt} = \frac{V_{mz} P}{K_{sz} + P} Z \tag{2.2}$$

The parameters of Michaelis-Menten curves are experimentally studied in our project team as displayed in Table 1. (principal investigator: Prof. T. Okaichi of Kagawa University supported by the special research programs on environmental science, Ministry of Education, Japan 1982-1984).

2.2 Numerical Results

Figure 3 shows vertical profiles of ecological compartments, E, P and Z in the case with no vertical migration by both phyto- and zooplanktons. The population of Chattonella antiqua (indicated by 'P') increases first at surface because of high light intensity (Figure 3-a). Then, the dense population moves to the point near the thermocline because of rich nutrient in the lower layer (Figure 3-b). However, after 57 hours, zooplankton prevails at all layers because its grazing exceeds the rate of primary production through the phytoplankton's photosynthesis (Figure 3-c). The vertical profiles of compartments E, P and Z are shown in Figure 4 in the case with migrations of both Chattonella antiqua and zooplankton. Chattonella antiqua moves upward during daytime and sinks during night and

zooplankton moves alternately upward during night and downward during daytime. In this case, the population of Chattonella antiqua increases greatly at surface like an outbreak of "red tide" (Figure 4-b). Chattonella antiqua is able to preserve its high growth rate around the layer of 11 meters depth, because it has little chance to encounter zooplanktons (Figure 4-c).

2.3 Discussion

These numerical results are quite easily understood if it is validated that Chattonella antiqua moves in completely alternate way with zooplankton's. However, this assumption hasn't yet got a solid support by the field study in this sea area. In the next section, let us take a vertical diffusion and upwelling of nutrients into the structure of two-dimentional ecological-hydrological model.

3 TWO-DIMENSIONAL MODEL

3.1 Model Structure

This model is constructed to investigate how the wind-induced zonal circulation gives its impact on the occurrence of "red tide". Figure 5 shows a schematic view of two-dimensional hydraulic model in terms of vertical profiles of temperature, salinity and nutrient. There is a thermocline at the depth of 20 meters. When wind blows in parallel with the coast at a constant speed of 10m/sec as illustrated in Figure 5, we have an upwelling stream of sea water in the left side of the costal zone and a down-stream in the right side.

The dynamics of the ecological compartments in this model is described by the terms of oceanographic transportation and biological interactions as shown in Figure 6:

$$\frac{\partial P}{\partial t} = -u\frac{\partial P}{\partial x} - w\frac{\partial P}{\partial z} + A_x\frac{\partial}{\partial x}(\frac{\partial P}{\partial x}) + A_z\frac{\partial}{\partial z}(\frac{\partial P}{\partial z}) + v_1(E)v_2(I)P - g(P)Z - \alpha P \tag{3.1}$$

$$\frac{\partial Z}{\partial t} = -u\frac{\partial Z}{\partial x} - w\frac{\partial Z}{\partial z} + A_x\frac{\partial}{\partial x}(\frac{\partial Z}{\partial x}) + A_z\frac{\partial}{\partial z}(\frac{\partial Z}{\partial z}) + g(P)Z - \beta Z \tag{3.2}$$

$$\frac{\partial E}{\partial t} = -u\frac{\partial E}{\partial x} - w\frac{\partial E}{\partial z} + A_x\frac{\partial}{\partial x}(\frac{\partial E}{\partial x}) + A_z\frac{\partial}{\partial z}(\frac{\partial E}{\partial z}) - v_1(E)v_2(I)P + \alpha P \tag{3.3}$$

$$\frac{\partial D}{\partial t} = -u\frac{\partial D}{\partial x} - w\frac{\partial D}{\partial z} + A_x\frac{\partial}{\partial x}(\frac{\partial D}{\partial x}) + A_z\frac{\partial}{\partial z}(\frac{\partial D}{\partial z}) + \beta Z \tag{3.4}$$

where u, w : horizontal and vertical current velocity,

A_x, A_z: horisontal and vertical eddy diffusivity,

$$v_1(E) = \frac{v_m E}{K_s + E},$$

$$v_2(I) = I(t)\exp(1.0 - \frac{I(t)}{I_{opt}}), \quad I_{opt} = \text{const.}$$

$$I(t) = \begin{cases} 1.0 \sin^3(\frac{\pi}{24}t)\exp(-0.01z) & : \text{day-time} \\ 0.0 & : \text{night} \end{cases}$$

$$g(P) = \begin{cases} R_m\left[1.0 - \exp\{\lambda(P^* - P)\}\right] & : \text{if } P^* \geq P \\ 0.0 & : \text{if } P^* \leq P \end{cases}$$

The model doesn't have any feedback loop from the detritus to other ecological compartment. In the long-run, this ecosystem will be composed of only detritus. However, since we are concerned with only the generation stage of the "red tide" for the period of two or three days, it is sufficient to take such a simple model structure as shown in Figure 6 for our numerical experiment.

3.2 Numerical Results

Figure 7 shows initial and the calculated zonal distributions of phytoplankton measured by chlorophyll-a (Chl.a) and nutrient PO -P. Our calculation begins at 6:00 in the morning. The Figure 7-a (10:00 on the first day) displays the increased Chl.a near the themocline where the nutrient is rich and light intensity is sufficient. At around 14:00 on the first day, the Chl.a increases rapidly near the coast up to the level of forming a "red tide" due to the coastal upwelling induced by wind which carries nutrients from bottom to surface (see Figure 7-b). In Figure 7-c (14:00 on the second day), the phytoplankton once increased near the coast is diffused during night toward offshore, and again the Chl.a will increase near the coast on the next day because of newly upwelled water rich in neutrient.

3.3 Discussion

The cycle of phytoplankton growth and decay can be explained in such a quantitative way as described in Figure 8. The term of "photosynthesis" of primary production, "grazing" of zooplankton and "advection" of transportation are shown in time axis in order to evaluate a material balance at the four specified points : 5 m depth and 3 km offshore, 5 m and 10 km, 15m and 3km, and 15m and 10 km, respectively. The term of photosynthesis changes its value according to the cyclic change of light intensity at 5 m or 15 m depth near coast or offshore. At the coastal point, the term of advection increases its negative value (transported to other region) with the development of coastal upwelling and other water movement (Figure 8-a). On the other hand, at the offshore point of 15 m depth, the photosynthetic term has a small value because of poor nutrient in the upper layer. The advection term has a positive value because of the supply from the lower layer

through coastal upwelling on the first day (Figure 8-b). On the second day, however, the advection term becomes negative (transported to other region) due to the influence of surface offshore current (Figures 8-a,c).

In this context, the existence of night may be important for the appearance of "red tide". Figure 9 shows the time-dependent zonal distributions of PO_4-P and the Chl.a in the case with no night. At first the Chl.a increases near the themocline where the nutrient and light are as sufficient as shown in Figure 7. The steady sunshine provides phytoplanktons with a sufficient photosynthesis capacity, in particular, at the place near the coast (where the upwelled nutrient exists) and the Chl.a increases like a "red tide" (Figures 9-b and 9-c). The experimental results by our model raise a question about the assumption that a vertial wind-induced upwelling along the coast can be a major factor which causes plankton blooms. Namely, the diffusive transportation during the night carries dense phytoplanktons up to the open sea area unless there is any up-and-down movement of planktons during the night. Thus both physical factors of phytoplankton movement and upwelling of sea water are essential to the development of a more realistic marine ecological model of "red tides".

4 THREE-DIMENSIONAL MODEL

4.1 Model structure

The three-dimensional model of two levels is constructed in order to simulate "red tides" which were observed on July 24, 1978 in Seto Inland Sea (see Figure 10). This model consists of two parts. One is to determine the tidal or wind-induced currents which are numerically calculated by Navier-Stokes type of fluid dynamic equations on tidal and wind forces in the Harima-Nada. The other is to calculate biological interactions among ecological compartments with diffusive and advective transportation in the

current field metioned above.

So far, a number of mathematical simulation models have been developed for describing a coastal marine ecosystem associated with "redtides" (Ikeda and Yokoi 1980, Kishi et al. 1980, Steel and Henderson 1977, Walsh 1977, and Wroblewski and O'Brien, 1976). These models are two-dimensional models either vertically or horizontally. Our previous discussion made it clear that it is important to consider both the vertical migrations of planktons and the horizontal transportation of all compartments by the water movement. Thus, we constructed the following three-dimensional ecological-physical model:

$$\frac{\partial}{\partial t} B = -\frac{\partial}{\partial x}(uB) - \frac{\partial}{\partial y}(vB) - \frac{\partial}{\partial z}((w+w_s)B) + \frac{\partial}{\partial x}(K_x \frac{\partial B}{\partial x}) + \frac{\partial}{\partial y}(K_y \frac{\partial B}{\partial y}) + \frac{\partial}{\partial z}(K_z \frac{\partial B}{\partial z}) + S_B, \quad (4.1)$$

where

u: a tidal current in the x-direction (cm/s)

v: a tidal current in the y-direction (cm/s)

w: a tidal current in the z-direction (cm/s)

w_s : speed of vertical migration (up-and-down) under light/dark cycle (cm/s)

K_x , K_y , K_z : coefficients of diffusion

S_B : a function which denotes biological interactions of compartment B

Dynamic equations on each ecological compartment B in the above general-equation are described as follows (see Figure 11):

$$S_{PH1} = (\mu_1(I,T) \cdot L_1(P,N) - M_1)PH1 - \frac{PH1}{PH1+PH2} v_Z(PH1, PH2)Z \quad (4-2)$$

$$S_{PH2}=(\mu_2(I,T)\cdot L_2(P,N)-M_2)PH1-\frac{PH2}{PH1+PH2}g_Z(PH1,PH2)Z \quad (4\text{-}3)$$

$$S_Z=(e_Z\cdot g_Z(PH1,PH2)-M_3)Z \quad (4\text{-}4)$$

$$S_{DP}=\{g_Z(PH1,PH2)\cdot(\frac{PH1\cdot\theta_{PH1,P}+PH2\cdot\theta_{PH2,P}}{PH1+PH2}-e_y\theta_{Z,P})+M_3\cdot\theta_{Z,P}\}Z$$
$$+M_1PH1\cdot\theta_{PH1,P}+M_2PH2\cdot\theta_{PH2,P}-\varphi DP \quad (4\text{-}5)$$

$$S_{DN}=\{g_Z(PH1,PH2)\cdot(\frac{PH1\cdot\theta_{PH1,N}+PH2\cdot\theta_{PH2,N}}{PH1+PH2}-e_y\theta_{Z,N})+M_3\cdot\theta_{Z,N}\}Z$$
$$+M_1PH1\cdot\theta_{PH1,N}+M_2PH2\cdot\theta_{PH2,N}-\varphi DN \quad (4\text{-}6)$$

$$S_P=-\mu_1(I,T)\cdot L_1(P,N)\cdot PH1\cdot\theta_{PH1,P}-\mu_2(I,T)\cdot L_2(P,N)\cdot PH2\cdot\theta_{PH2,P}$$
$$+(e_y-e_z)\cdot g_Z(PH1,PH2)\cdot Z\cdot\theta_{Z,P}+\varphi DP+O_P \quad (4\text{-}7)$$

$$S_N=-\mu_1(I,T)\cdot L_1(P,N)\cdot PH1\cdot\theta_{PH1,N}-\mu_2(I,T)\cdot L_2(P,N)\cdot PH2\cdot\theta_{PH2,N}$$
$$+(e_y-e_z)\cdot g_Z(PH1,PH2)\cdot Z\cdot\theta_{Z,N}+\varphi DN+O_N \quad (4\text{-}8)$$

Definitions of symbols and variables in these equations are as follows:

$PH1$= concentration of *Chattonella* as measured by its carbon content (μgC/l)

$PH2$= a concentration of Diatoms as measured by its carbon content (μgC/l)

Z= a concentration of zooplankton as measured by its carbon content (μgC/l)

DP= a concentration of detritus as measured by its phosphorus content (μgP/l)

DN= a concentration of detritus as measured by its nitrogen content (μgN/l)

P= a concentration of dissolved inorganic phosphorus (μgP/l)

N= a concentration of dissolved inorganic nitrogen (μgN/l)

where S_{PH1}, S_{PH2}, S_Z , S_{DP} , S_{DN} , S_P and S_N represent increase or decrease of Chattonella antiqua, phytoplanktons of other types, zooplankton, detritus in phosphorus, detritus in nitrogen, inorganic phosphorus and inorganic nitrogen in the sea water, respectively.

μ (I,T) (i=1,2) is a function of photosynthesis in the following type:

$$\mu_i(I,T)=\mu_{imax}\frac{T}{T_{iopt}}exp(1-\frac{T}{T_{iopt}})\cdot\frac{1}{\Delta h}\int_{layer}\frac{I(z)}{I_{iopt}}exp(1-\frac{I(z)}{I_{iopt}})dz \tag{4-9}$$

$$I(z)=I_0exp(-kz) \tag{4-10}$$

where

μ_{imax}= the maximum photosynthesis rate of *Chattonella* or Diatoms (1/day)

I= light intensity at z (ly/day)

k= extinction coefficient (1/m)

$I_0(t)$= light intensity at the surface (ly/day)

$$I_0 = \begin{cases} I_{max}sin^3((\pi/DL)t) & (daytime) \\ 0 & (nighttime) \end{cases} \tag{4-11}$$

DL= a daytime period (s)

T= water temperature (°C)

I_{iopt}= the optimum light intensity for photosynthesis (ly/day)

T_{iopt}= the optimum water temperature for photosynthesis (°C)

All ecological parameters and the initial values of each compartment are shown in Table 3 and 4.

4.2 Numerical results

The calculated tidal residual currents are shown in Figure 12. There is a clockwise current in the northern part of the Harima-Sea, and counter-clockwise currents in the southern part. They are quite in good accordance with the observed data concerning the constant flow in the upper layer of the sea as displayed in Figure 13. Figure 14 illustrates the combined case of tidal and wind-induced current residual. The tidal boundary conditions at the Bisan-Seto and the Kii-Channel and other physical parameters are described in Tables 5 and 6.

As far as the distributional profiles of nutrients are concerned, the portion of their high concentration is located around the loading points of nutrients because of their diffusive nature (see Figure 15). However, the horizontal distribution of Chattonella antiqua (the mean value in 24 hours on the third day from the initial state) is quite different from the distributional pattern of the nutrients as shown in Figure 16. Figures 17-a and 18-a are the distributions of Chattonella antiqua at the upper layer with and without wind force, respectively, and Figures 17-b and 18-b are also those at the lower layer, respectively.

In the case with no wind, the dense population of Chattonella antiqua can be seen at the center of Harima-Sea and Osaka Bay (Figure 17-a). In the case with wind, however, the densely populated area moves toward the eastern direction, because wind-induced currents transport the plankton paches to the eastern direction in the upper layer (Figure 18-a). In the lower layer, there is no dense patches of "chattonella antiqua" due to the vertical migration of the phytoplankton (Figures 17-b and 18-b). However, the phytoplankton of other types such as Diatom (S_{PH2}) has a more dense population than "Chattonella antiqua" at the northern part of the Harima-Sea (Figure 19). These results are in comparatively good agreement with the field observation on July 24, 1978 which detected a large scale of "red tide" at the eastern part of Harima-Sea as is schematically shown in Figure 10 (Okaichi 1982).

4.2 Discussions

The calculated results shown here are the daily mean value on the third day of the calculation started from the uniform initial state. The numerical values of initial state displayed in Table 4 are assummed to be a kind of the steady-state solutions where the ecosystem reached already some

steady conditions. The additional nutrient inputs from rivers, winds or tides will change that steady-state into a different steady-state (see Figures 14-18). To get a new steady-state solution in such a large area, it takes an enormous amount of computation interval, for example, at least more than 20 days in terms of stabilization of the computation. Hence it should be noted that the results shown here describe only some of the transient states after three days from the uniform state. For the analysis of "red tide" outbreaks, it would be extremely important to have such good parameter values in the ecological-hydrological structure that could stabilize a computation scheme of Eqs. (4.1) -(4.8) within the blooming interval of several days.

5 CONCLUSION

The research project of "red tides outbreaks in Japanese coastal waters" started in 1979, headed by Professor T. Okaichi of Kagawa University. Since then, much effort has been made to obtain numerical values of biological parameters that are supposed to associate with the generation mechanism of "red tide" (Okaichi 1982 and 1984). Using such values of biological parameters and physical conditions studied by other members of the project team, we construct a system of simulation models.

The numerical experiments carried out by our three models have shown that :

i) The amount of nutrients and oceanographic characteristics of the sea are basic factors for a rapid increase of phytoplankton population.

ii) The alternate migration of both phyto- and zooplanktons in the vertical direction according to a light/dark cycle causes a dense phytoplankton population in the upper layer.

iii) The tidal current plus the water movement induced by the wind has a great impact on phytoplankton dynamics.

However, we have not yet tested other cases where factors of inorganic or metallic matters such as vitamine B_{12} and ferrus from bottom deposit are taken into the mechanism of "red tide" outbreak. Although it is widely accepted that those factors have an important part in the primary production, it is extremely difficult to establish a quantitative relationship between those factors and the growth-rate function. There has been little field suties on this problem except a few pioneer works (Nakamura and Watanabe 1983, Hata and Nishijima 1982). We must further make sure the impacts of these uncertain factors on the generation mechanism of "red tide" through both numerical experiments and field observations.

ACKNOWLEDGEMENT

This study is supported by the special research program on the "environmental science" funded by the Ministry of Education, Japan. We wish to express our sincere thanks to Professor Toshiyuki Hirano, University of Tokyo for his guidance in developing our modeling work, and also to Mr. Hajime Nishimura, graduate student, Kyoto University, for his valuable assistance in conducting the computer simulations. Our gratitudes are also due to all members of the project team of "red tides" problem headed by Professor Tomoyuki Okaichi, Kagawa University.

REFERENCES

Hata, Y. and Nishijima, T., 1982. Distribution of aerobic heterotrophic bacteria and B group vitamines in Harima-Sea, Report on "Fundamental studies on the effects of marine environment on the outbreaks of red tides", Research report on Env. Sci. B148-R14-8. Min. of Education, Japan.

Iizuka, S.,1980. Red Tide - Occurrence mechanism and control, The Japanese Soc. of Fisheries. Series 34, Koseisha Koseikaku Pub. (in Japanese).

Ikeda, S. and Yokoi, T.,1980. Fish population dynamics under nutrient enrichment. Ecological Modelling, 10: 141-165

Kishi, M.J., Nakata, K. and Ishikawa, K.,1981. Sensitivity analysis of coastal marine ecosystems. J. Oceanogr. Soc. Japan, 37: 120-134.

Nakamura, Y. and Watanabe, M., 1983. Growth characteristics of Chattonella antiqua, J. Oceanogr. Soc. Japan, 39: 110-114.

Okaichi, T. (ed.), 1982. Foundamental studies on the effect of marine environment on the outbreaks of red tides. Research report on Env. Sci. B148-R14-8. Min. of Education, Japan.

Okaichi, T.,1983. Marine environmental studies on outbreaks of red tides in neritic waters. J. Oceanogr. Soc. Japan, 39.

Okaichi, T. (Ed.), 1984. Fundamental studies on the modeling of ecophysical environment in relation with red tides. Research report on Env. Sci. (to appear). Min. of Education, Japan.

Steel, J. and Henderson, E., 1977. Plankton patch in the North Sea in "Fishery Mathematics" (ed. by J. Steel), Academic Press.

Walsh J., 1977. A biological sketchbook for an eastern boundary current, in "The Sea" vol.:Marine Modeling, Wiley-Interscience.

Wroblewski, J.S., O'Brien, J.J.,1976. A spatial model of phytoplankton patchiness. Mar.Biol., 35:357-394.

Yanagi, T., 1982. The ocean characteristics and their change in the Seto Inland Sea, La mer, 20:170-177.

Table 1 Biological parameters in one-dimensional model and initial values of ecological compartments

Vm (maximum photosynthetic rate)		2.0 ^{1}/day
Ks (half saturation const.)		1.0 μg-at. PO_4-P/l
Vmz (maximum grazing rate)		1.5 μg-C/μg-C copepoda/day
Ksz(half saturation const. in grazing)		193 μg-C/l
W (vertical migration velocity)		2.0 m/hour
initial values		
E (PO_4-P)	upper layer	0.1 μg-at. P/l
	lower layer	0.7 μg-at. P/l
P (Chatonella. antigua)		2.0 μg-chl.a/l
Z (Paracalanus. parvus)		15.0μg-C/l

Table 2 Biological parameters in the two-dimensional model and initial values of ecological compartment

Vm (maximum photosynthetic rate)		1.0 ^{1}/day
Ks (half saturation const.)		1.0 μg-at. PO_4-P/l
Rm (maximum grazing rate)		0.5 μg-C/μg-C copepoda/day
(limiting const. in grazing)		0.02 (μg-C/l)
P* (limiting const. in grazing)		5.0 μChl-a/l
w (vertical migration velocity)		2.0 m/hour
α and β (mortality rates)		0.2 ^{1}/day
C/Chl-a (carbon/chlorophyll-a)		30.0 μ-C/μ-Chl-a
C/P (carbon/phosphorus)		15.0
initial values		
E (PO_4-P)	upper layer (z > 15m)	4.5 μg-at. P/l
	lower layer (z < 15m)	0.0 μg-at. P/l
P (Chatonella. antigua)		5.0 μg-chl.a/l
Z (Paracalanus. parvus)		15.0 μg-C/l

Table 3 Parameter values used in eco-physical computations

symbols	definitions	values
μ_{1max}, μ_{2max}	the maximum photosynthesis rate	2.0 (1/day)
K_{P1}	the half saturation constant	10.0 (μgP/l)
K_{N1}		108.8 (μgN/l)
K_{P2}		12.8 (μgP/l)
K_{N2}		108.6 (μgN/l)
$\theta_{PH1,P}$	a weight conversion rate of *Chattonella*	1.58E-2
$\theta_{PH1,N}$		1.91E-1
$\theta_{PH2,P}$	a weight conversion rate of Diatoms	2.13E-2
$\theta_{PH2,N}$		1.81E-1
I_{1opt}, I_{2opt}	the optimum light intensity for photosynthesis	150.0 (ly/day)
T_{1opt}, T_{2opt}	the optimum water temperature for photosynthesis	25.0 (degree Celsius)
DL	a daytime period	0.5
I_{max}	the maximum light intensity	600.0 (ly/day)
k	extinction coefficient	1.28E-1 (1/m)
g_{Zmax}	the maximum grazing rate of zooplankton	2.0 (1/day)
λ	the ivlev constant	2.0E-3
e_y	a assimilation efficiency	0.7
e_z	a gross growth efficiency	0.3
$\theta_{Z,P}$	weight conversion rate of zooplankton	1.57E-2
$\theta_{Z,N}$		1.97E-1
M_1, M_2	mortality rates of phytoplanktons	0.1 (1/day)
M_3	a natural death rate of zooplankton	0.1 (1/day)
φ	a bacterial decomposition rate of detritus (the bottom)	3.5E-2 (1/day)
		5.5E-5 (1/day)
w_{Pmax}	the maximum migration speed of *Chattonella*	3.5E-2 (cm/s)
w_{Zmax}	the maximum migration speed of zooplankton	2.1E-2 (cm/s)
K_x, K_y	diffusion coefficients	1.0E6
K_z		0.1

Table 4 Initial values used in eco-physical computations

symbols	definitions	values
P	inorganic phosphorus	7.0 μgP/cm^3
N	inorganic nitrogen	65.0 μgN/cm^3
$PH1$	*Chattonella*	60.0 μgC/cm^3
$PH2$	Diatoms	60.0 μgC/cm^3
Z	Zooplankton	3.5 μgC/cm^3
DP	phosphorus in detritus	10.0 μgP/cm^3
		6.5 mgP/cm^2 (the bottom)
DN	nitrogen in detritus	120.0 μgN/cm^3
		0.5 mgN/cm^2 (the bottom)

Table 5 Boundary conditions used in tidal current computations

symbols	definitions	values
(Bisan Seto)		
ζ_0	a height of a mean surface	0.0 cm
A	amplitude of tidal current from outside	89.0 cm
ω	angular velocity	8.333E-3 degree/sec
K	phase angle	90.0 degree
(Kii Channel)		
ζ_0	a height of a mean surface	0.0 cm
A	amplitude of tidal current from outside	42.0 (Shikoku) - 46.0 (Wakayama) cm
ω	angular velocity	8.333E-3 degree/sec
K	phase angle	-63.0 (Shikoku) - -55.0 (Wakayama) degree

Table 6 Parameter values used in tidal current computations

symbols	definitions	values
γ_a^2	a drag coeffifient	1.3E-3
γ_i^2	a interlayer friction coefficient	1.3E-3
γ_b^2	a bottm friction coefficient	2.6E-3
ρ_a	the air density	1.3E-3 (g/cm^3)
f	the coliolis parameter	8.32E-5 (rad/s)
A_H	a eddy friction coefficient	1.0E5 (cm^2/s)
K_x, K_y	eddy diffusion coefficients	1.0E5 (cm^2/s)
K_z		5.0E-2 (cm^2/s)

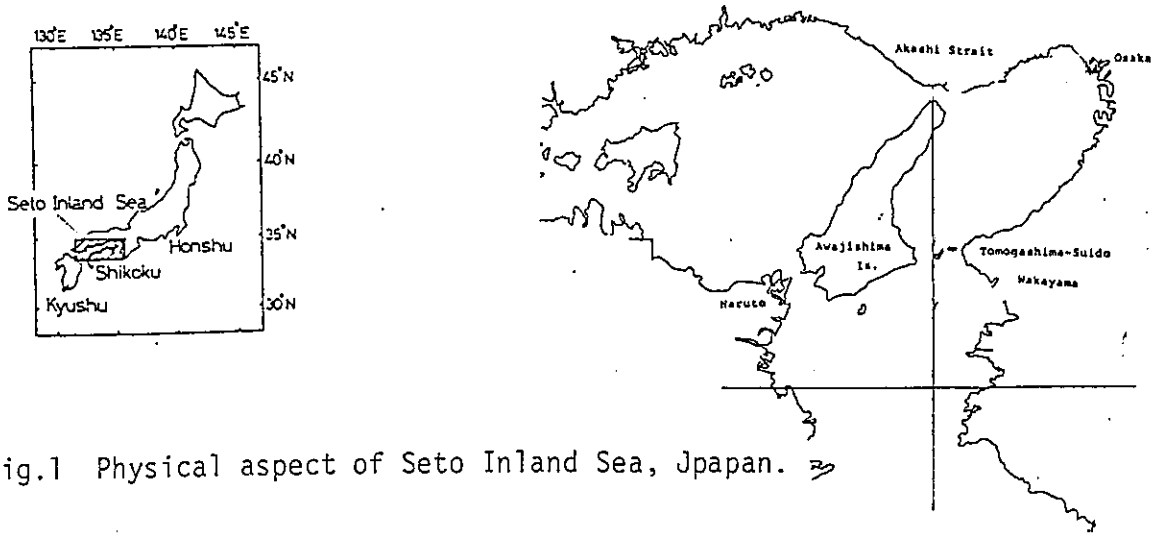

Fig.1 Physical aspect of Seto Inland Sea, Jpapan.

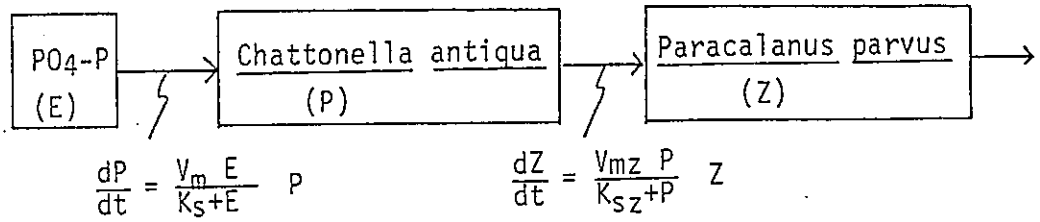

Fig.2 Relations of biological process in one dimensional model.

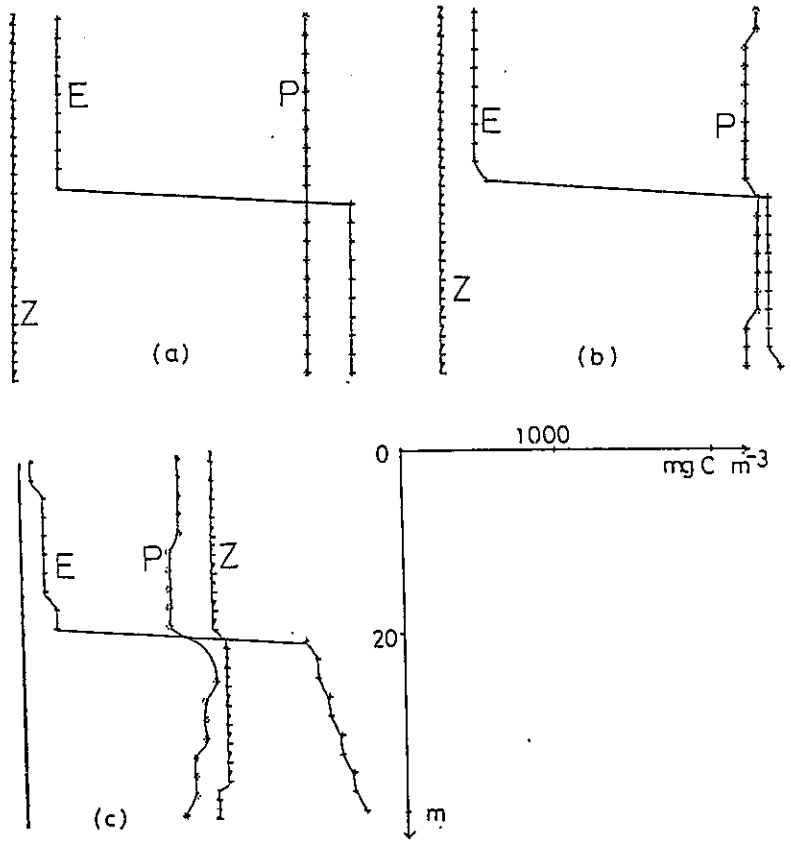

Fig.3 Vertical profiles of E, P and Z without vertical migrations.
a.initial states(6:00) b.9 hours after initial states(15:00)
c.81 hours after initial states(15:00 on 4th day)

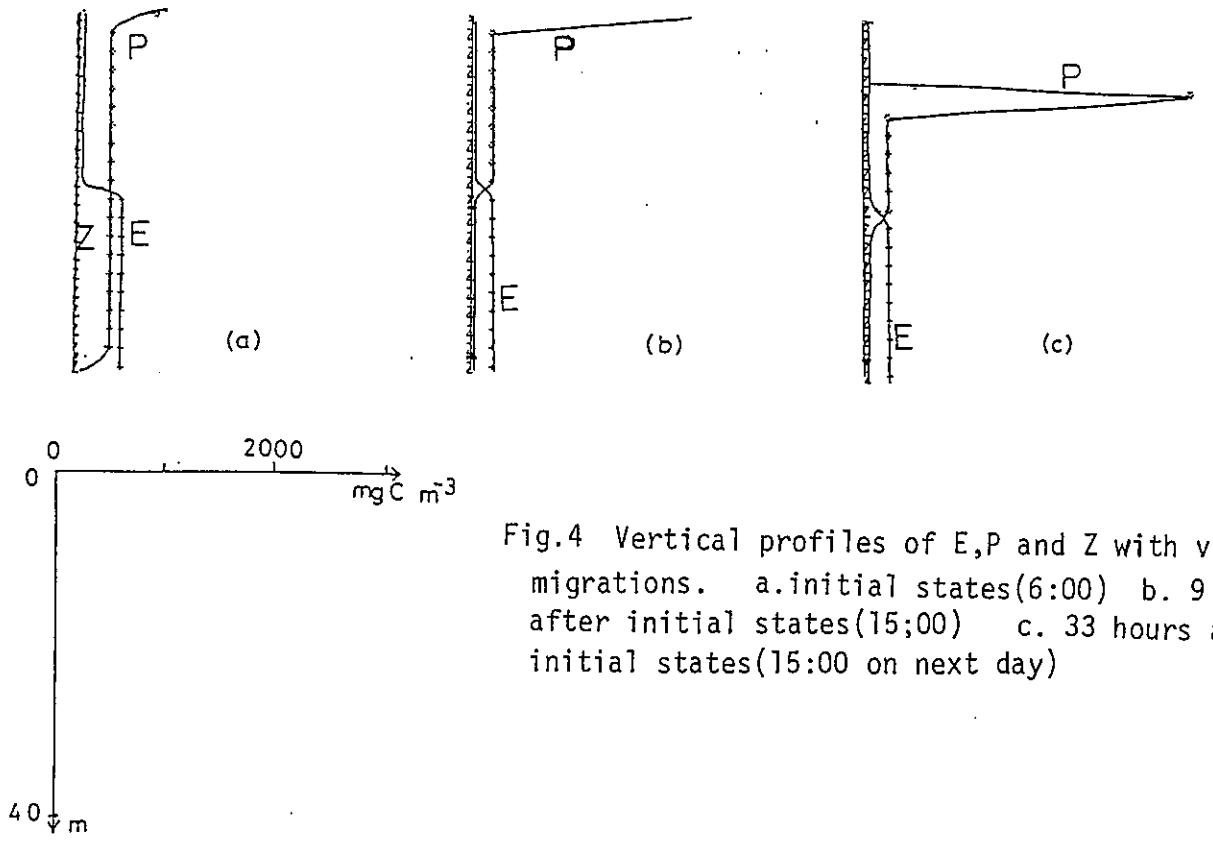

Fig.4 Vertical profiles of E,P and Z with vertical migrations. a.initial states(6:00) b. 9 hours after initial states(15;00) c. 33 hours after initial states(15:00 on next day)

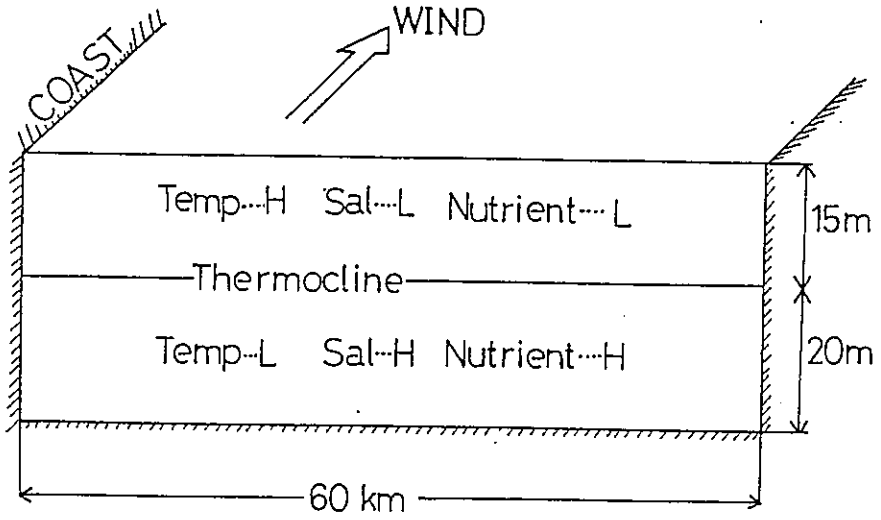

Fig.5 A schematic view of two dimensional model.

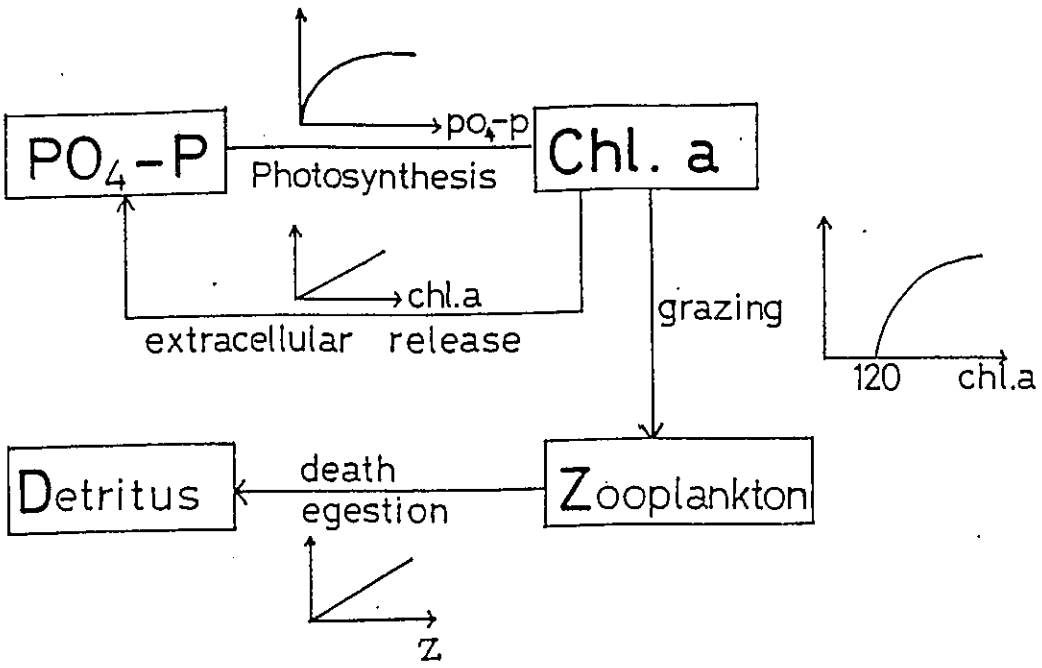

Fig.6 Relations of biological process in a two dimensional model.

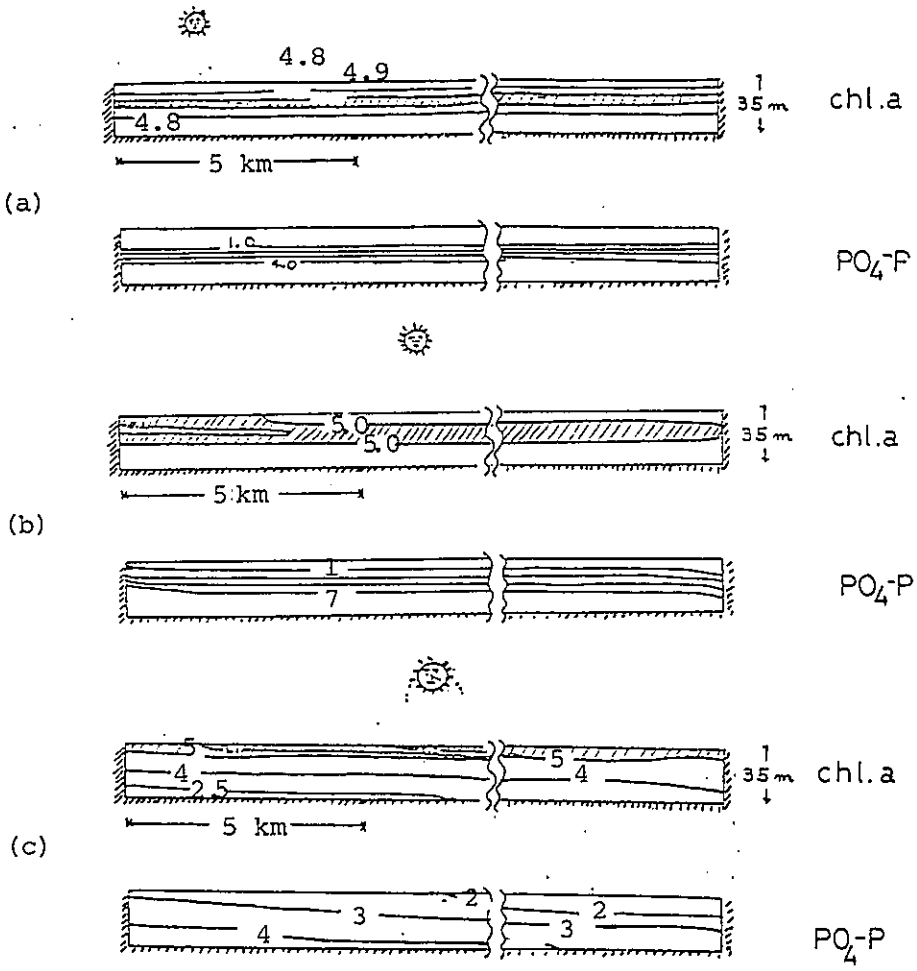

Fig.7 Zonal distributions of PO4-P and chl.a in two dimensional model. (a)4 hours after initial states(10:00) (b)8 hours after(14:00) (c)32 hours after (14:00 on the next day) ,unit PO4-P:μg at.PO_4-P l^{-1} chl.a:mg chl.a l^{-1}

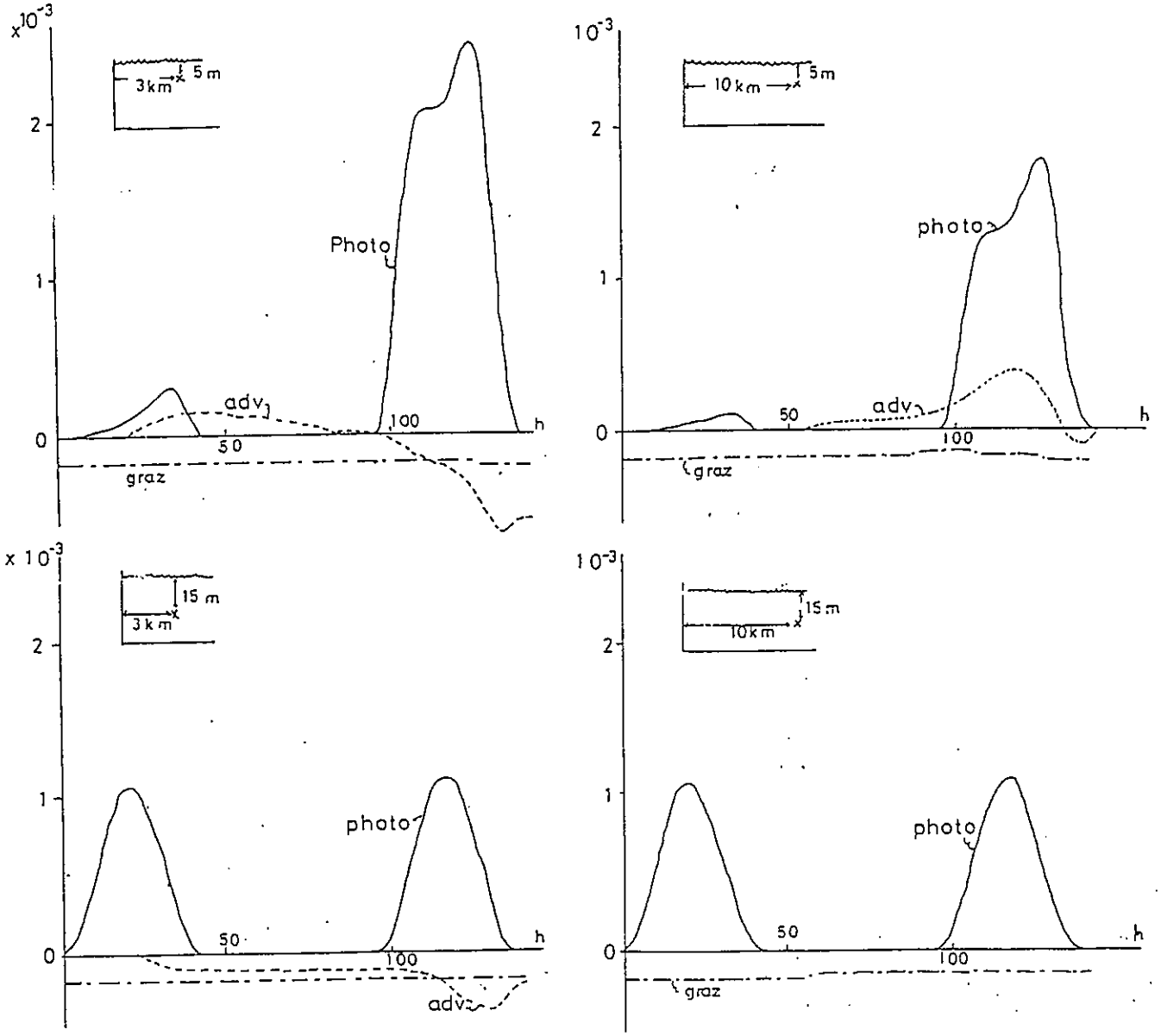

Fig.8 Time changes of each term in diffusion equation.
solid line:photosynthesis, dotted line:advection, dashed line:grazing mortality. unit:mg C m^{-3} h^{-1}

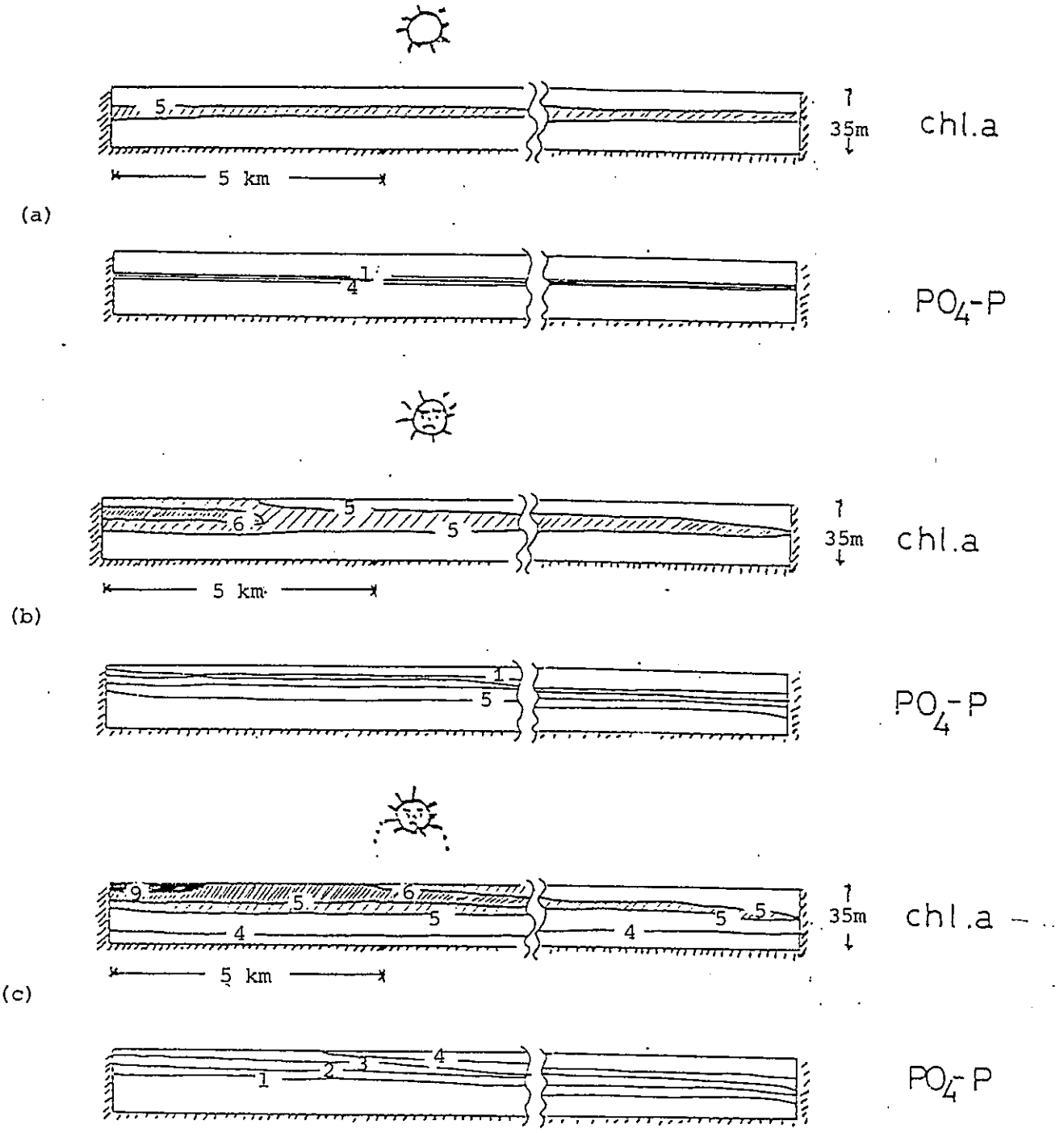

Fig.9 Zonal distributions of PO_4-P and chl.a in the case without night.
(a) 4 hours after initial states (10:00) (b) 12 hours after
(c) 24 bours after

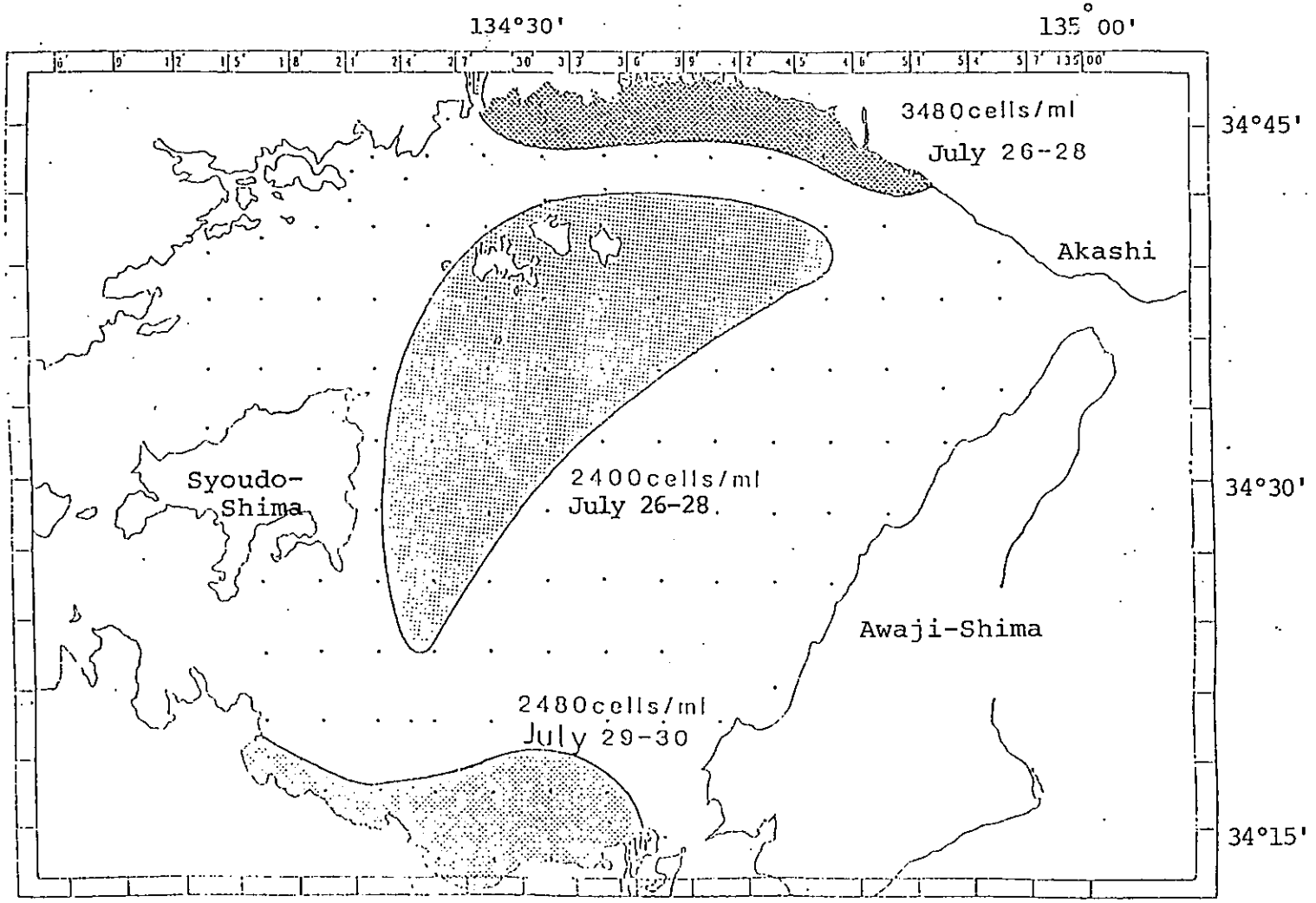

Fig.10 Schematic Illustration of the observed red tides on July, 1978 (Okaichi 1982)

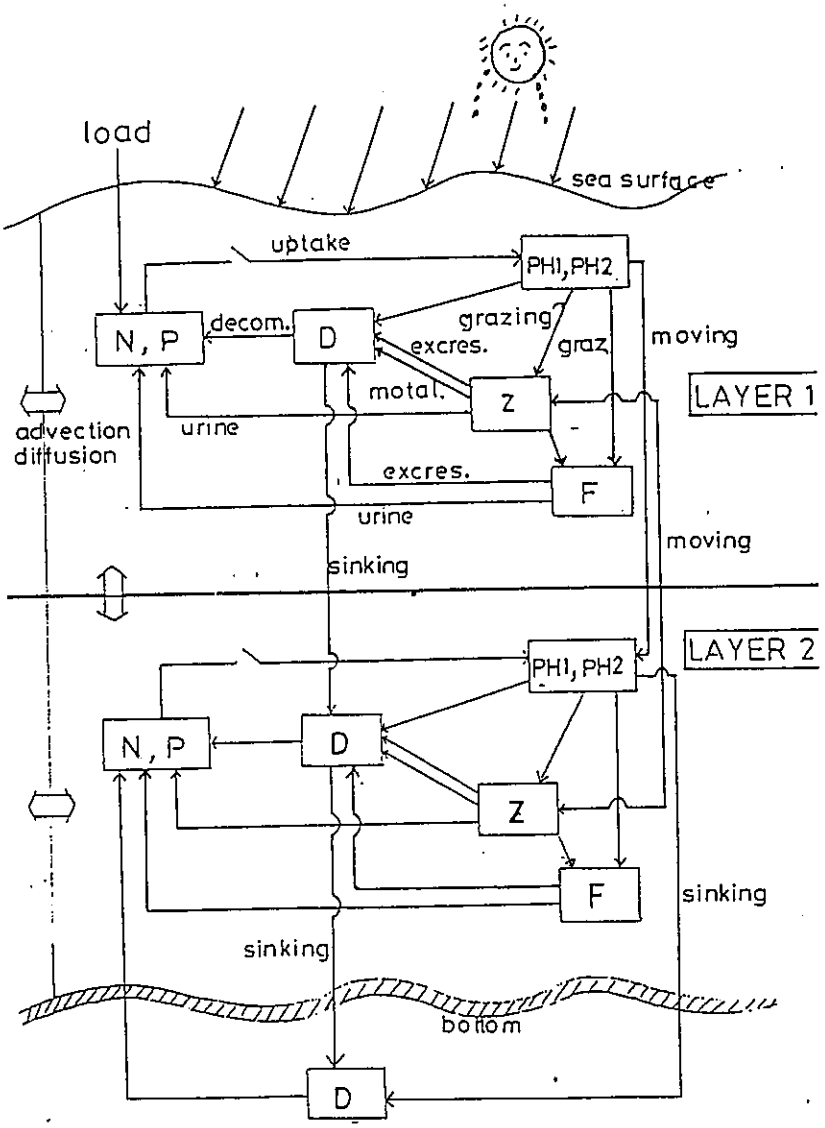

Fig.11 Schematic view of three dimensional model. In this case two leveled.

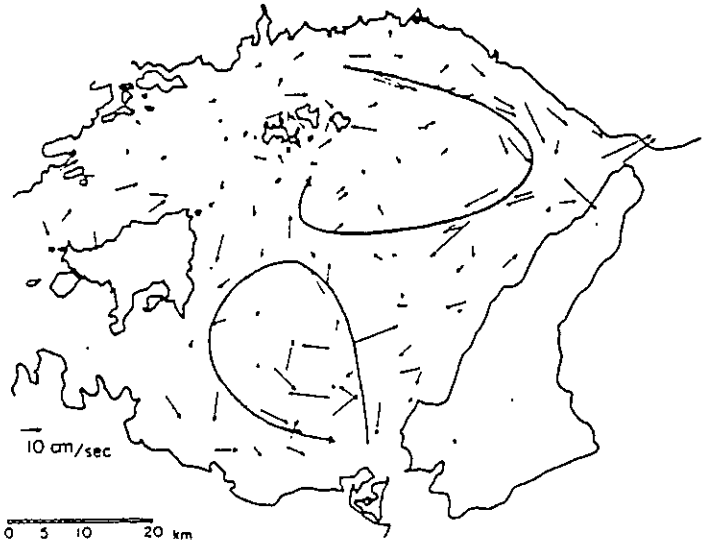

Fig. 13 Contant flow in the upper of the Harima Sea
(Yanagi 1982)

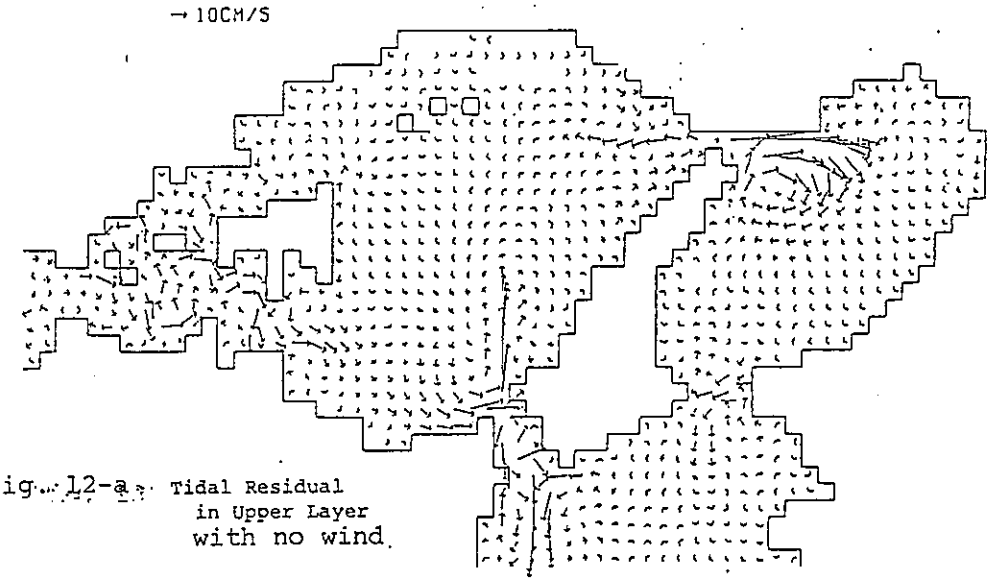

Fig. 12-a Tidal Residual in Upper Layer with no wind.

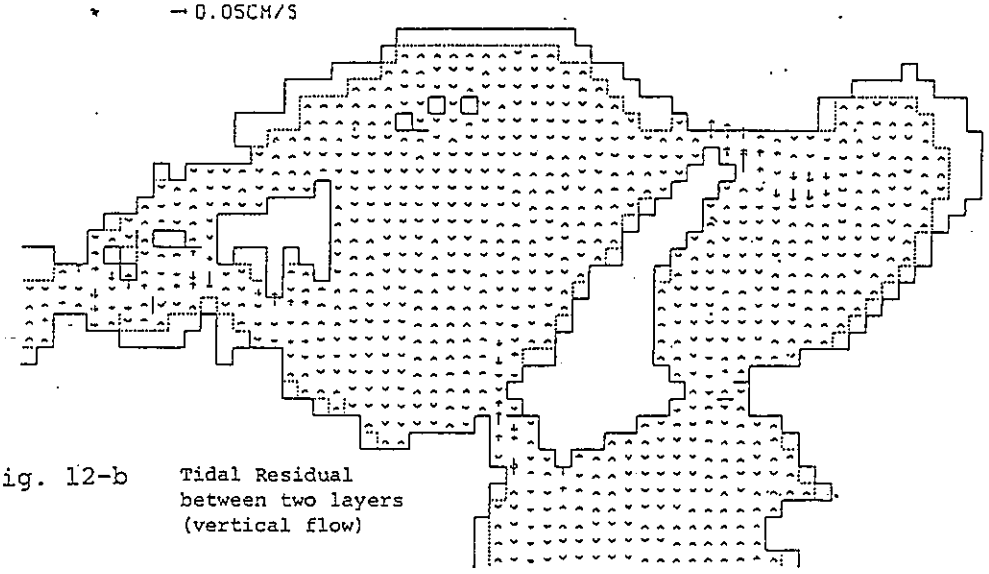

Fig. 12-b Tidal Residual between two layers (vertical flow)

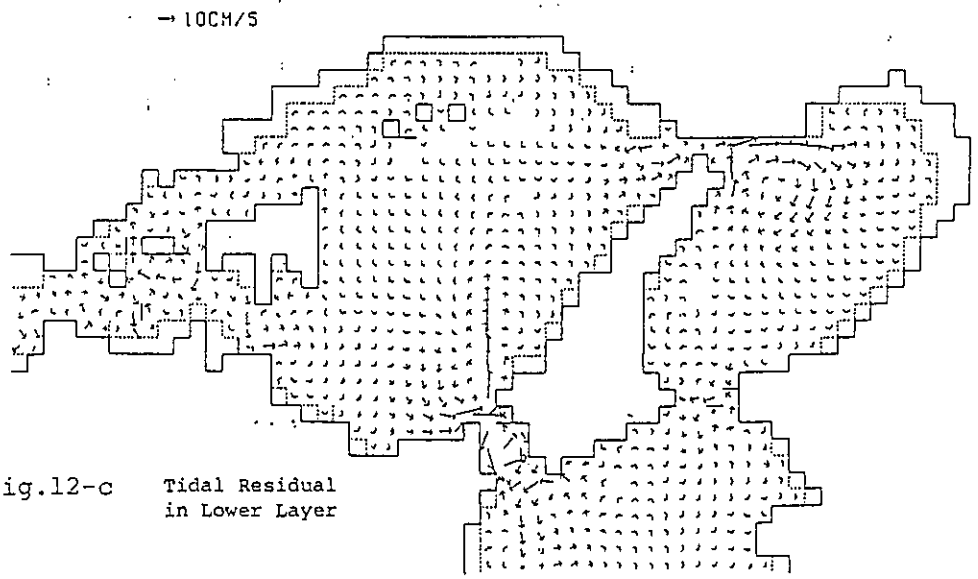

Fig.12-c Tidal Residual in Lower Layer

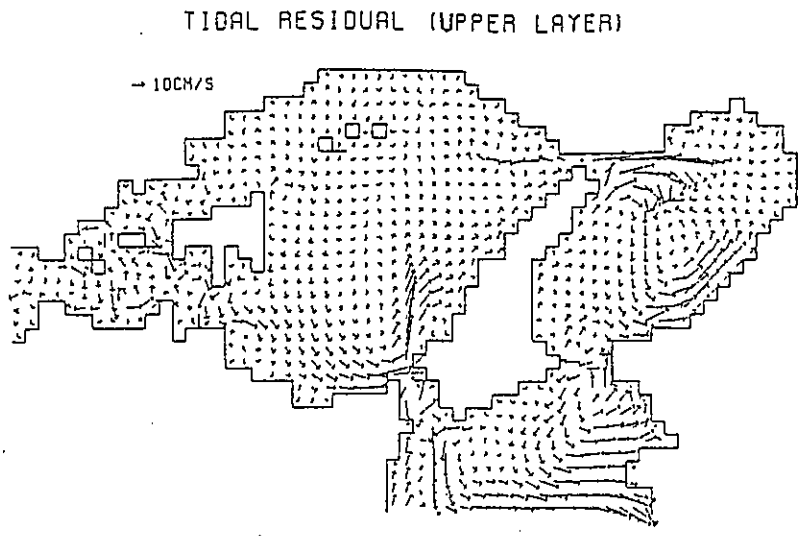

Fig.14 Calculated tidal residual current in Harima-nada in the case with wind shown below (daily mean)

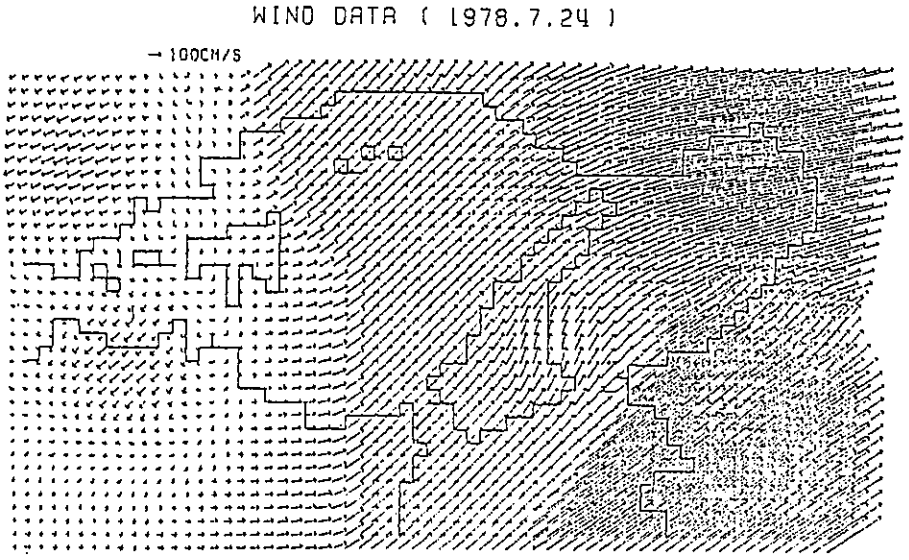

Calculated sea surface wind based on the data of meteorological stations on Jun. 24 1978.

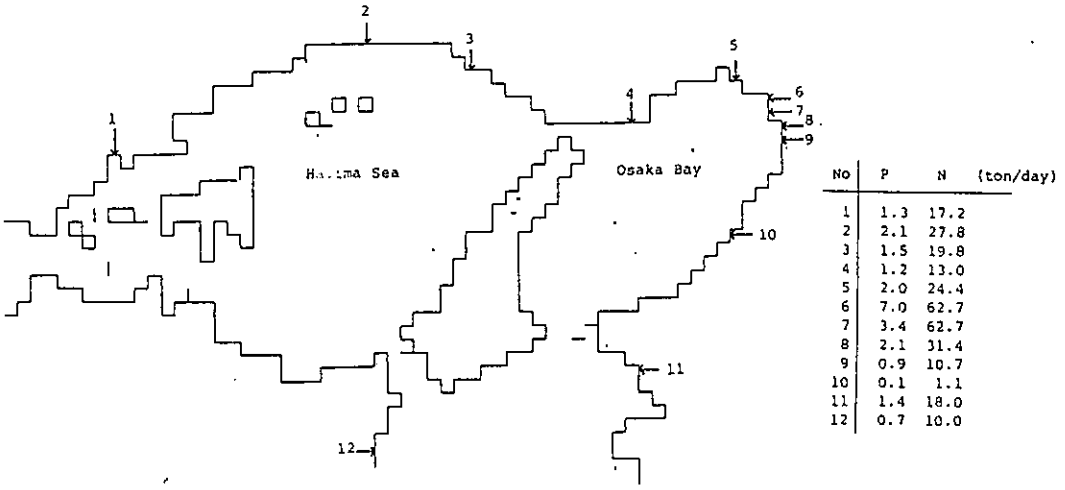

No	P	N	(ton/day)
1	1.3	17.2	
2	2.1	27.8	
3	1.5	19.8	
4	1.2	13.0	
5	2.0	24.4	
6	7.0	62.7	
7	3.4	62.7	
8	2.1	31.4	
9	0.9	10.7	
10	0.1	1.1	
11	1.4	18.0	
12	0.7	10.0	

Fig. 15 Nutrient loads and loading points

Fig.16(a) DISTRIBUTION OF INORGANIC P (LAYER 1)

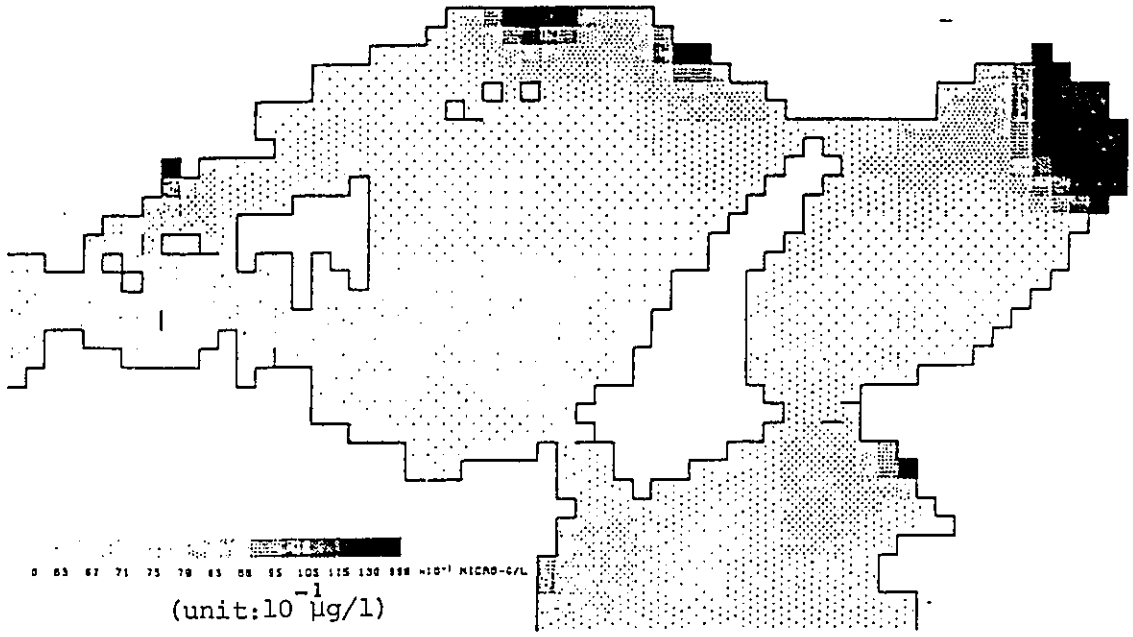

(unit:10^{-1}µg/l)

Fig.16(b) DISTRIBUTION OF INORGANIC P (LAYER 2)

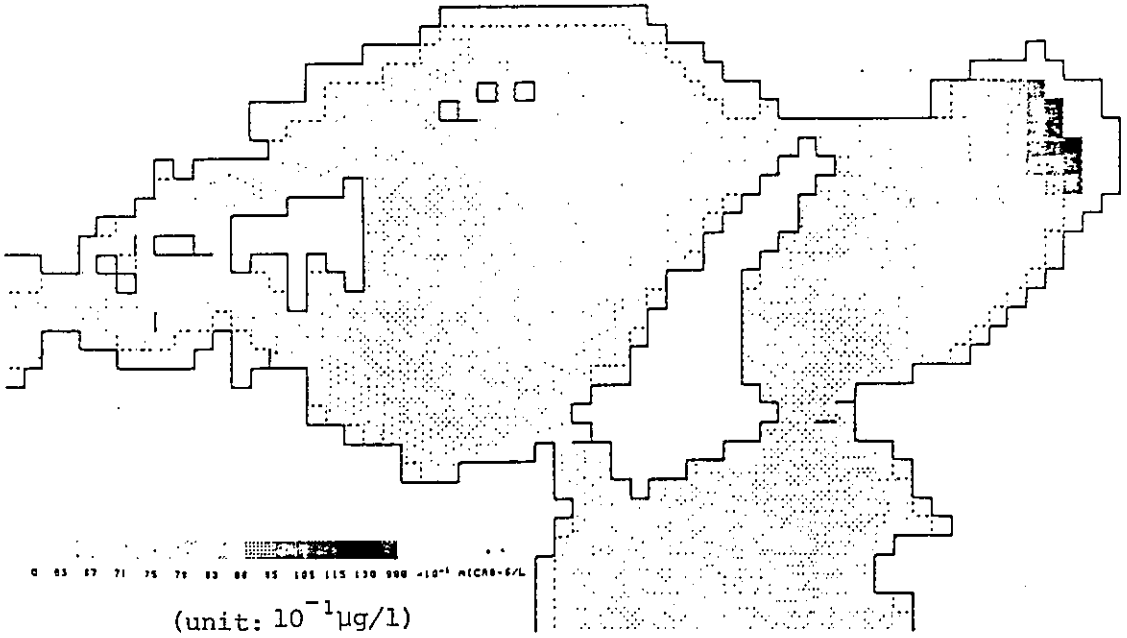

(unit: 10^{-1}µg/l)

Fig.16(c) DISTRIBUTION OF INORGANIC N (LAYER 1)

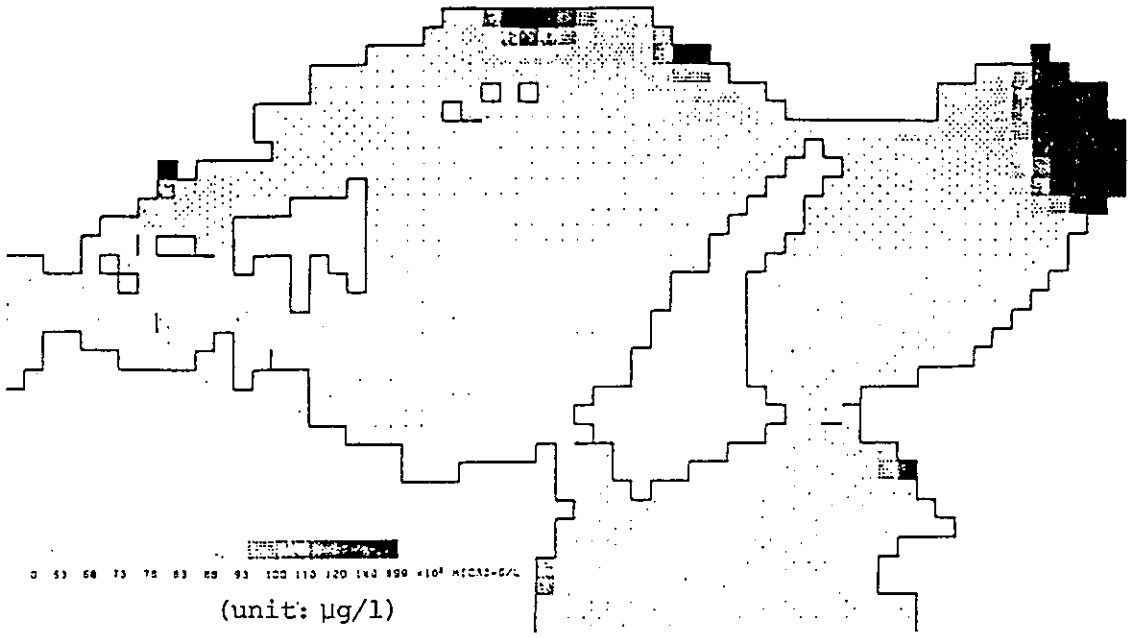

(unit: µg/l)

Fig.16(d) DISTRIBUTION OF INORGANIC N (LAYER 2)

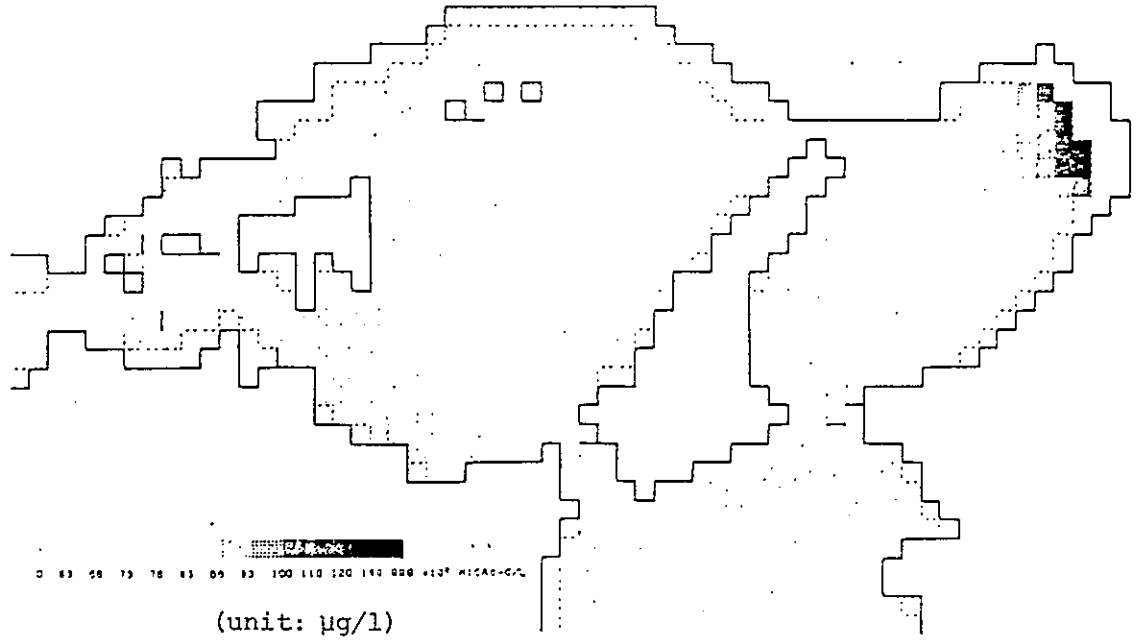

(unit: µg/l)

Fig. 17-a DISTRIBUTION OF CHATTONELLA (LAYER 1)

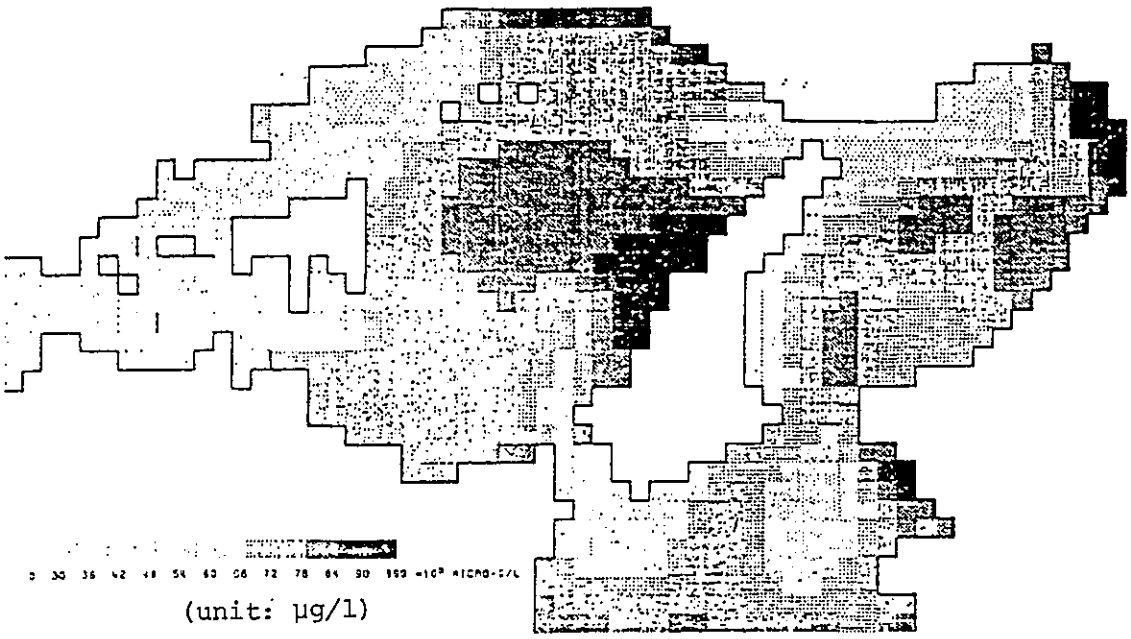

(unit: µg/l)

Fig. 17-b DISTRIBUTION OF CHATTONELLA (LAYER 2)

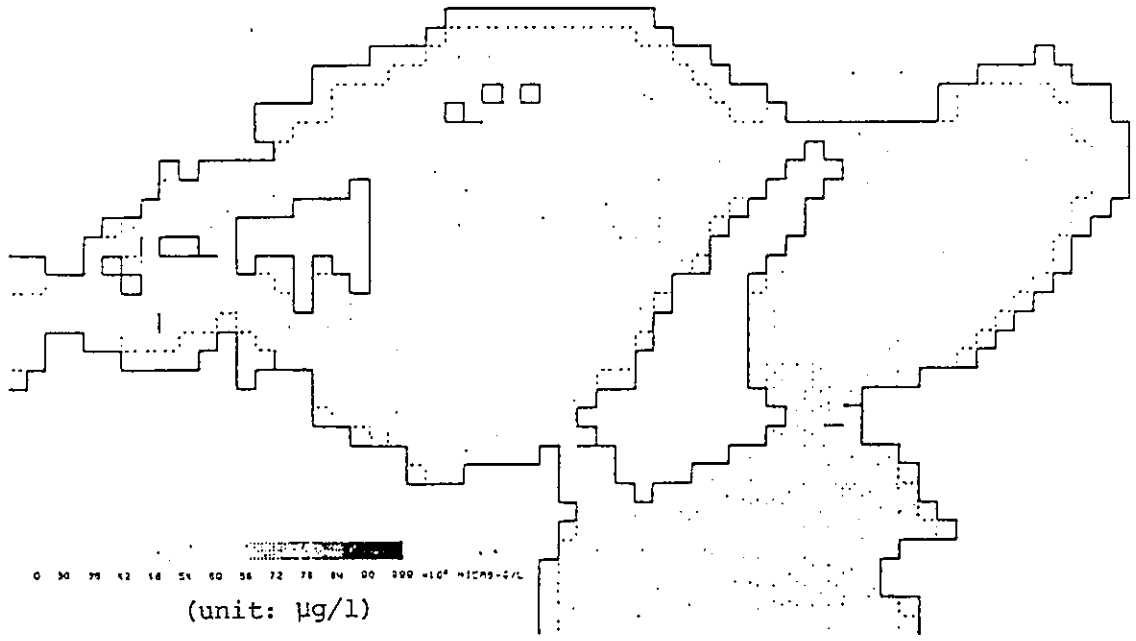

(unit: µg/l)

Fig.18-a DISTRIBUTION OF CHATTONELLA (LAYER 1)

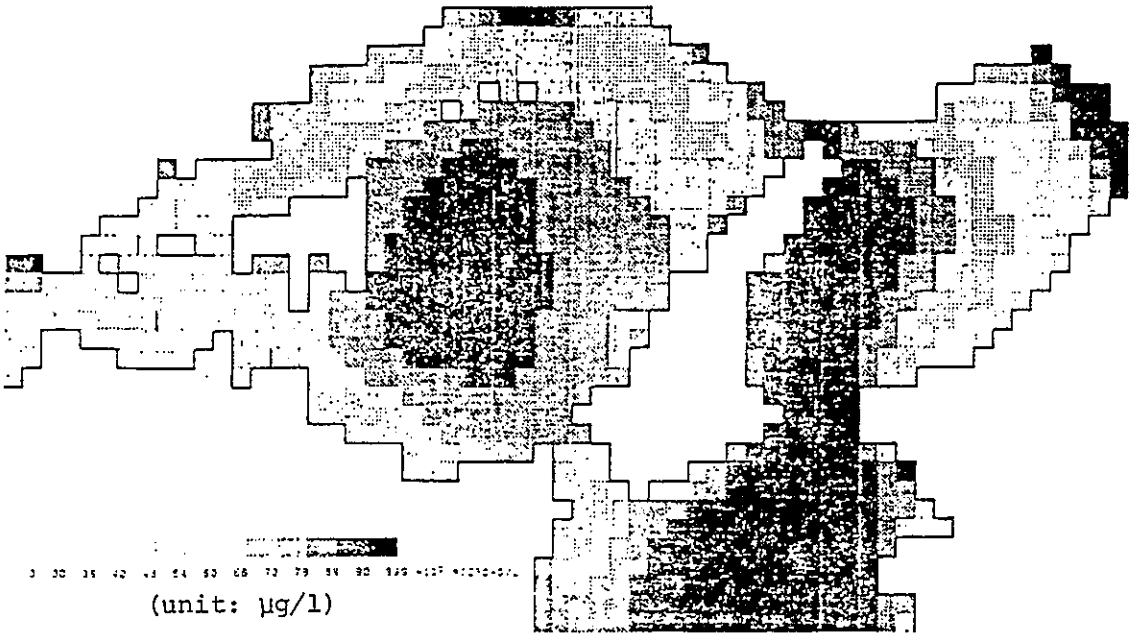

(unit: µg/l)

Fig.18-b DISTRIBUTION OF CHATTONELLA (LAYER 2)

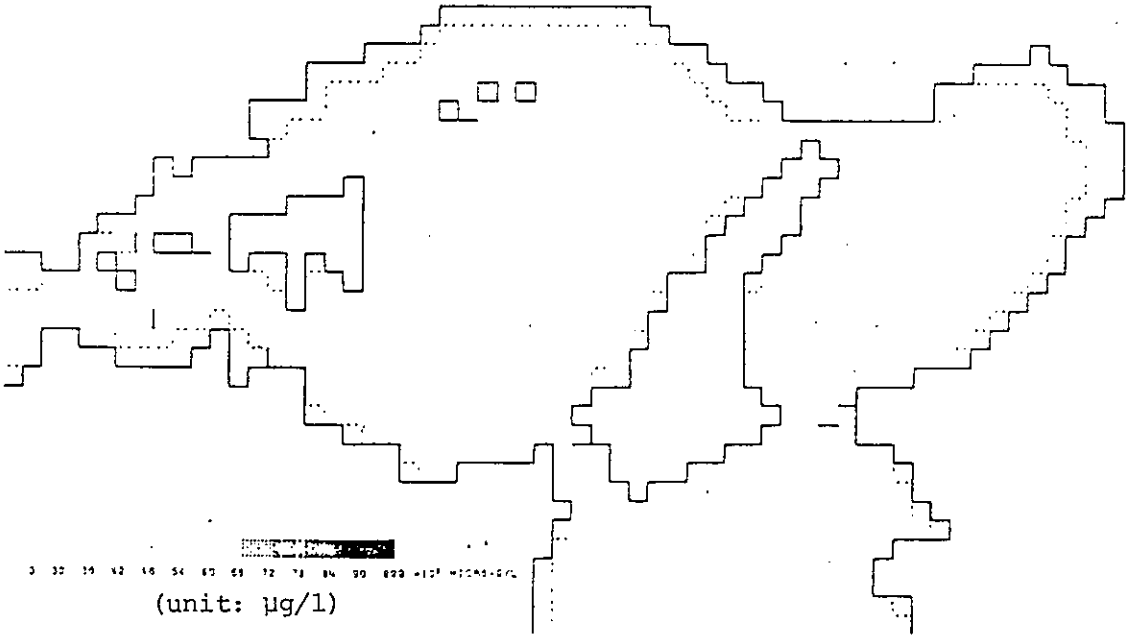

(unit: µg/l)

Fig.17 Distribution of Components (Case C)

Fig. 19-a DISTRIBUTION OF DIATOMS (LAYER 1)

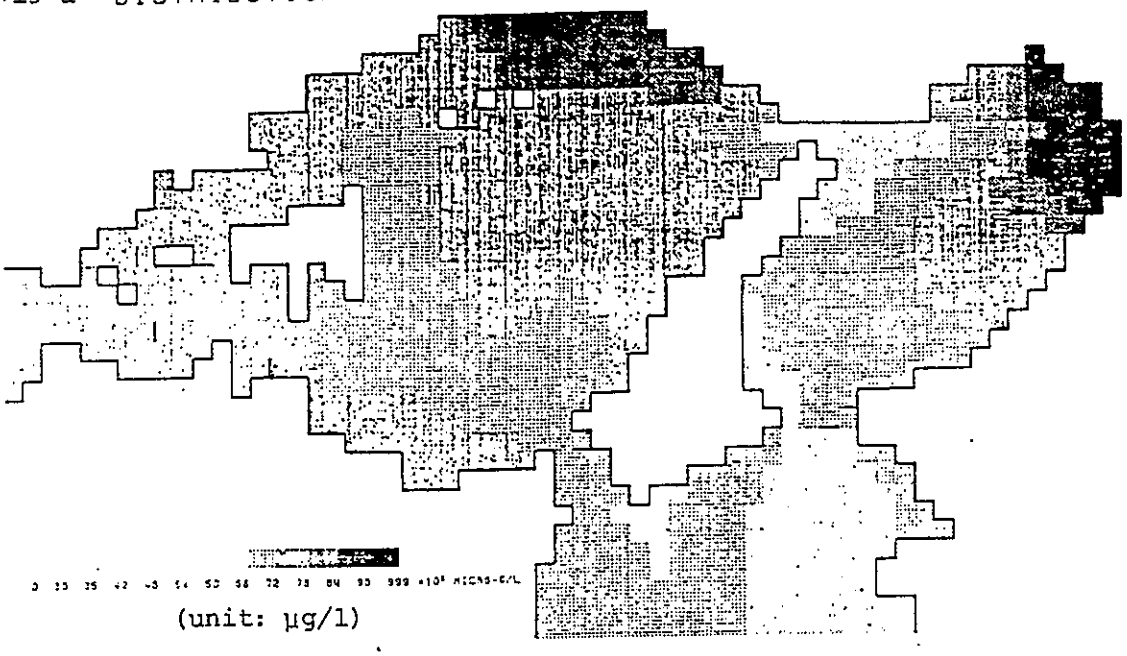

(unit: µg/l)

Fig. 19-b DISTRIBUTION OF DIATOMS (LAYER 2)

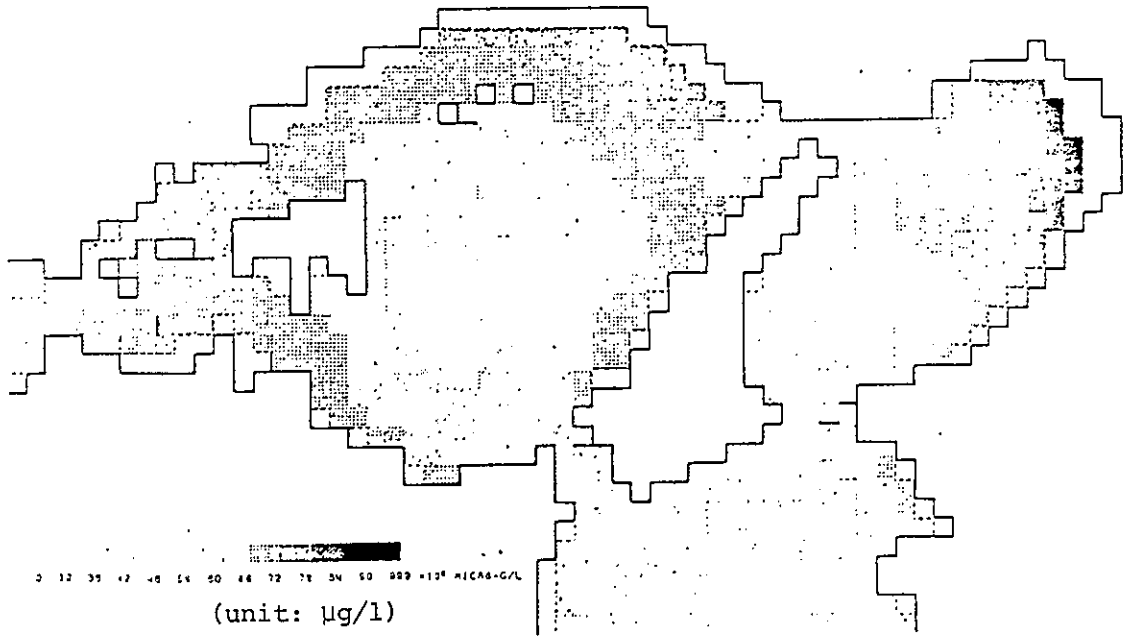

(unit: µg/l)